ELSEVIER

Nuclear Instruments and Methods in Physics Research B 192 (2002) 206–214

NIM B
Beam Interactions with Materials & Atoms

www.elsevier.com/locate/nimb

Positron and electron total cross sections for collisions with C_2F_6 and $C_2H_3F_3$ molecules

O. Sueoka *, C. Makochekanwa, H. Kawate

Faculty of Engineering, Institute of Applied Science, Yamaguchi University, Tokiwadai 2-16-1, Ube, Yamaguchi 755-8611, Japan

Abstract

The experimental total cross sections (TCSs) data for 0.7–600 eV positrons and 0.8–600 eV electrons colliding with hexafluoroethane (C_2F_6) and 1,1,1-trifluoroethane ($C_2H_3F_3$) molecules are presented. These data are compared with the data of ethane (C_2H_6) measured previously. On the positron TCS data below 5 eV, the TCS curves are quite different from each other. For energies 7–25 eV, the data for these three kinds of molecules are comparable, though above 60 eV the C_2F_6 TCS data are roughly twice those of C_2H_6. The $C_2H_3F_3$ TCS data have magnitudes almost midway between those of C_2F_6 and C_2H_6. The TCS curves for electrons show the same variation with energy as the positron data above 60 eV. In the low energy region, a few weak resonant peaks are observed in the C_2F_6 and $C_2H_3F_3$ electron TCS curves. On the electron TCS data in the range 5.5–14 eV, the C_2F_6 data are lower than the C_2H_6 data.

PACS: 34.80.Bm; 34.80.Gs; 36.10.Dr
Keywords: Positron scattering; Electron scattering; Positronium (Ps) formation; Total cross section; Ethane-related molecule

1. Introduction

Because of their strong relation to the reactive plasma process, studies of electron–gas collisions have greatly progressed [1]. Hexafluoroethane (C_2F_6) gas is used in laboratories and factories as an etching gas in the reactive plasma process. The study of electron scattering from C_2F_6 molecules contributes the fundamental data for controlled processes in the reactive plasma. Though the study of electron scattering from C_2F_6 is important, not enough has been done yet. Takagi et al. [2] have measured the differential cross sections (DCSs) for electrons colliding with C_2F_6 for impact energies from 2 to 100 eV and scattering angles from 10° to 130°. They obtained the integral and momentum transfer cross sections, and the energy loss spectra by vibrational excitation. In this paper, the electron TCS data for C_2F_6 are also compared with those of Szmytkowski et al. [3] for energies 0.5–250 eV and Sanabia et al. [4] for energies 0–20 eV. For $C_2H_3F_3$ however, we have neither electron nor positron TCS data for comparison. Christophorou et al. have compiled and discussed on the various electron scattering data of C_2F_6 [5].

In the present paper, we report the data on the total cross section (TCS) measurements for 0.7–600 eV positrons and 0.8–600 eV electron

* Corresponding author. Tel.: +81-836-359972/859806; fax: +81-836-359492/859801.
E-mail addresses: osueoka@po.cc.yamaguchi-u.ac.jp, osueoka@yamaguchi-u.ac.jp (O. Sueoka).

0168-583X/02/$ - see front matter
PII: S0168-583X(02)00870-4

scattering by C_2F_6 and 1,1,1-trifluoroethane ($C_2H_3F_3$). $C_2H_3F_3$ is a polar molecule. The measured TCS values for C_2H_6 and C_2F_6 are corrected by eliminating the forward scattering effect, whilst the correction has not been performed for $C_2H_3F_3$. The effect of imperfect treatment of the forward scattering is discussed later. The electron TCS data of C_2F_6 are discussed in comparison with the C_2F_6 TCS data of Szmytkowski et al. [3], Sanabia et al. [4], the integral cross section (ICS) data of Takagi et al. for C_2F_6 [2], and the TCS data for CH_4 [6] and CF_4 [7]. The experimental results are compared with those of C_2H_6 for the discussion of the effect of hydrogen and fluorine atoms. The positron TCS data for C_2F_6 and $C_2H_3F_3$ are compared with the positron TCS data for C_2H_6 [6], CH_4 [6] and CF_4 [7]. Positronium (Ps) formation cross section at 2 eV above the threshold energy of Ps formation, E_{Ps}, was measured by our group's method [8]. The results are discussed as ratios of the positronium cross section (Q_{Ps}) to the TCS (Q_t) using other data obtained previously [8]. A preliminary report on the positron and electron scattering by C_2F_6 was presented before [8,9].

2. Experimental procedure

2.1. Apparatus and projectiles

A ^{22}Na radioisotope with an activity of 65–85 Ci was used for the positron source. A set of conventional tungsten (W) ribbons baked at 2100 °C was used for the positron beam moderator. The energy width of the positron beam is typically 2.3 eV (FWHM). On the other hand, slow electron beams with an energy width of around 1.4 eV (FWHM) are produced, after the same W moderator moderates secondary electrons that are emitted from the same radioisotope, through multiple scattering.

The apparatus for the TCSs for positron and electron scattering is a straight type TOF with a flight length of 600 mm. A schematic diagram of the experimental set-up is shown in Fig. 1. A retarding potential unit is included in the TOF apparatus as an energy selector for positron and electron beams. This unit is located in front of the beam detector, ceratron, as shown in Fig. 1. The

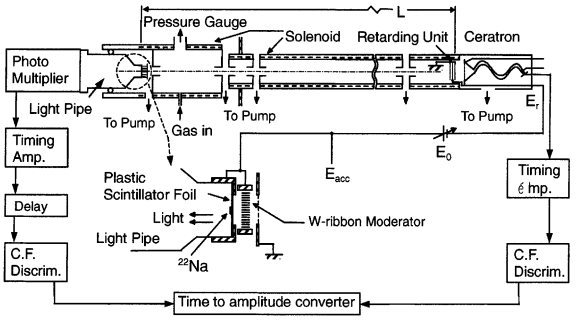

Fig. 1. Schematic diagram of the experimental arrangement. The abbreviated symbols, E_r, E_{acc}, E_0 and C.F.Discrim are retarding energy, acceleration energy, constant energy ($E_0 = E_{acc} - E_r$) and constant fraction discriminator, respectively.

retarding potential is applied for eliminating the beam intensity contributions from large energy-loss inelastic scattering, and for decreasing elastically scattered and/or small energy loss such as via vibrational and rotational excitation scattered contributions with reduced axial velocities. For the main measurements, the same acceleration potential (E_{acc}), 1.0 eV lower than E_{acc} for positron beams, was applied for electron beams as the retarding potential. The purities of the specimen gases C_2H_6, C_2F_6 and $C_2H_3F_3$ were 99.7%, 99.999% and 99%, respectively.

2.2. Total cross section measurements

TCS values, Q_t are derived from the following equation.

$$Q_t = (-1/nl)\ln(I_g/I_v), \quad (1)$$

where n is gas density in the collision cell, l is the effective length of the collision cell which is derived from the normalization of our positron-N_2 data to the experimental positron-N_2 TCS data of Hoffman et al. [10]. That is, the TCSs are decided relatively. I_g and I_v are the beam intensities in the gas and vacuum runs, respectively. The beam intensities are obtained by the analysis method of Mori and Sueoka [11], which was derived from the original one of Coleman et al. [12].

In order to ensure the independence of the effective length l of the collision cell on the cell

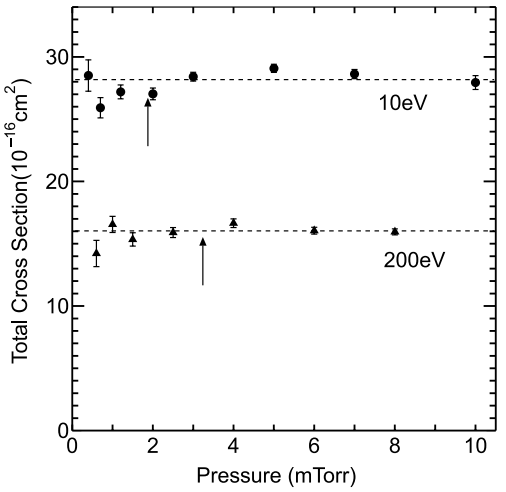

Fig. 2. TCSs, for C_2F_6, plotted against gas pressure for 10 eV and for 200 eV. The arrows indicate the pressure at a beam intensity attenuation I_v/I_g of 3. The error bars show the statistical and the density fluctuation error only.

pressure, other TCS measurements for electron collision were performed. As shown in Fig. 2, no variation showing the pressure dependence of TCSs for C_2F_6 is observed. This has been the case with every other previous study by our group.

2.3. Magnetic field and forward scattering correction

A magnetic field parallel to the flight path is applied using solenoid coils for the beam transportation as shown Fig. 1. The beam intensity strongly depends on the field strength since the perpendicular component of the beam velocity to the flight path depends on the magnetic field. Therefore, it is necessary to use as weak a magnetic field as possible. Besides, the exit aperture of the collision cell is very wide, being 3 mm in radius. According to the above conditions of this apparatus, the measured raw cross section data are fairly affected by forward scattering effects.

The forward scattering correction is performed by the method described previously [13]. The DCS data used in this correction are the experimental electron scattering data of Takagi et al. for C_2F_6 [2] and of Tanaka et al. for C_2H_6 [14], where the DCS data are not perfectly covered in all the necessary energy and angle regions, extrapolated values from the experimental DCS are used in the calculation. Because no DCS data exist in positron scattering for these molecules, the electron DCS data were also used for correcting the positron data.

In the correction, the TCS Q_t is obtained as

$$Q_t = Q_{t(\text{measured})} + Q_f, \tag{2}$$

where Q_f is the cross section due to forward scattering and is obtained by integration over all the angles between 0 and the maximum angle θ_{max} against the DCSs, $q(\theta)$. This process is complicated in practice, because the diameter of the aperture of the collision cell, R, is very large, and the magnetic field B is applied there too. The forward scattered intensity, I_f, was obtained by a simulation calculation using the following equation.

$$I_f = \frac{1}{\pi R^2 Q_t}\int_0^{\ell} dI(x)\int_0^{R} 2\pi r\,dr \times \int_0^{\theta_{max}} \Phi(\theta, r, x, E, B) q(\theta)\sin\theta\,d\theta, \tag{3}$$

where $dI(x)$ is the scattered intensity between x and $x + dx$, x is the position coordinate parallel to the flight path and r the radial position coordinate. The function Φ is the transmission function and is a function of B (magnetic field intensity), E (beam energy), r, x, R and the effective collision cell length l. Q_f is obtained from I_f using the following relation,

$$Q_f = I_f Q_t / I_s, \tag{4}$$

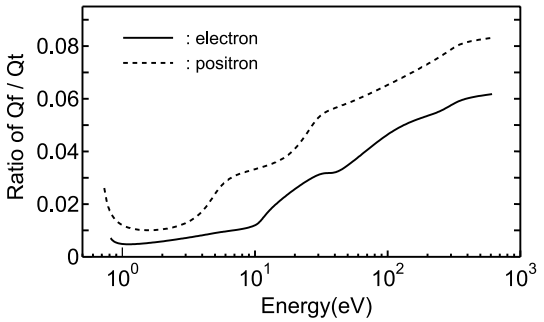

Fig. 3. The ratio of the forward scattering cross section to the TCS values for C_2F_6; (– – –): positron scattering; (—): electron scattering.

where I_s is the total scattered intensity. The resultant correction ratios of the forward scattering cross section to the TCS, Q_f/Q_t, for the data of C_2F_6 are plotted in Fig. 3.

3. Experimental results

The TCSs for 0.7–600 eV positrons and 0.8–600 eV electrons colliding with C_2F_6 and $C_2H_3F_3$ were relatively measured. The data for $C_2H_3F_3$ are not corrected for the forward scattering effect, because there is no DCS data. The TCS data for C_2F_6 and $C_2H_3F_3$ are shown in Figs. 4 and 5, respectively. The TCS numerical values for positron and electron scattering by C_2F_6 and $C_2H_3F_3$ molecules are shown, together with the associated total errors, in Tables 1 and 2.

The error, as the total uncertainty, is estimated by addition of $\Delta n/n$, $\Delta l/l$ and $\Delta I/I$. Here I means $\ln(I_v/I_g)$, and ΔI includes all statistical errors in the counting. The value of $\Delta I/I$ is around 2% for positron collision and less than 0.5–1% for electron collision. The error in the gas density, Δn, is almost solely due to the sensitivity of the pressure gauge (CMH4-M11 of Vacuum General); $\Delta n/n$ is around 0.3% depending on the collision gas pressure. The error due to the normalization procedure for the determination of the effective length $\Delta l/l$ was estimated to be 3%. The error in the experimental data of Hoffman et al. [10] is not included in the error, Δl. Moreover, the error in the procedure for the forward scattering correction is not included also.

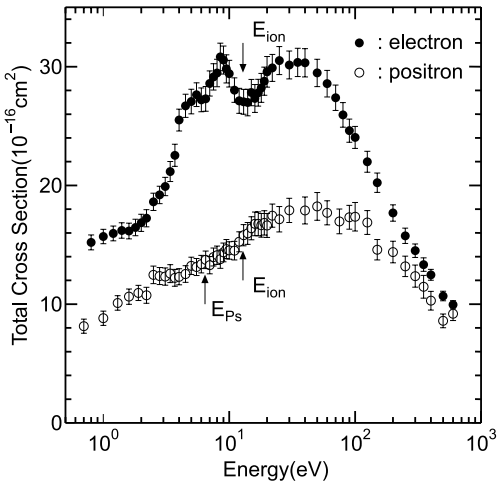

Fig. 4. TCSs for positron and electron impact on hexafluoroethane (C_2F_6). Error bars show the total uncertainties. Arrows indicate the thresholds for Ps formation (E_{Ps}) and ionization (E_{ion}).

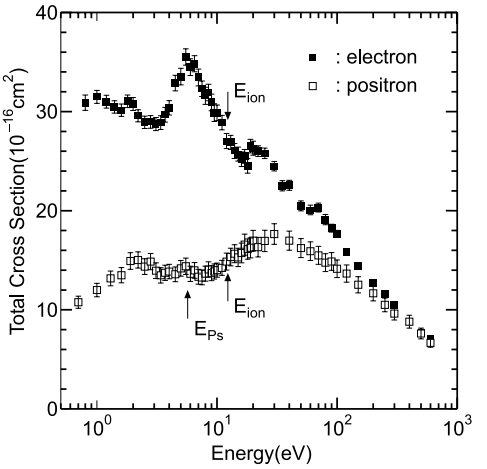

Fig. 5. TCSs for positron and electron impact on 1,1,1-trifluoroethane ($C_2H_3F_3$). Error bars show the total uncertainties. Arrows indicate the thresholds for Ps formation (E_{Ps}) and ionization (E_{ion}).

The positron data of C_2F_6 and $C_2H_3F_3$ in the energy range below 20 eV are plotted together with the TCS data for C_2H_6 [6], CF_4 [7] and CH_4 [6] in Fig. 6. The data for CF_4 and CH_4 are corrected for the effect of forward scattering. The data corrected for forward scattering effects are larger by around 5% than the previous data, as shown in the case of C_2F_6 in Fig. 3. A small hump is observed at around 2.5 eV in the C_2F_6 data. The TCS values for C_2F_6 are almost equal to those for $C_2H_3F_3$ and C_2H_6, though the TCSs for C_2H_6 increase with decreasing impact energy below 2.5 eV. It can be seen that the relationship between the data for CF_4 and CH_4 is roughly the same with that between the data for C_2F_6 and C_2H_6. In the TCS data for $C_2H_3F_3$, a distinct peak is seen at 2.1 eV. The origin of the peak is unknown. For energies 5–20 eV, the TCS values for $C_2H_3F_3$ are very close to those for C_2F_6. For energies 8–20 eV,

Table 1
TCSs (10^{-16} cm^2) for positrons and electrons colliding with C_2F_6 (the errors are the total uncertainties in the text)

Positron				Electron			
E (eV)	TCS	E (eV)	TCS	E (eV)	TCS	E (eV)	TCS
0.7	8.2 ± 0.6	15	16.4 ± 1.0	0.8	15.2 ± 0.7	13	27.0 ± 1.1
1.0	8.8 ± 0.6	16	16.8 ± 1.0	1.0	15.7 ± 0.7	14	27.0 ± 1.2
1.3	10.1 ± 0.7	17	16.5 ± 1.0	1.2	16.0 ± 0.7	15	27.8 ± 1.2
1.6	10.6 ± 0.7	18	16.6 ± 1.0	1.4	16.2 ± 0.7	16	27.3 ± 1.2
1.9	10.9 ± 0.7	19	16.9 ± 1.1	1.6	16.2 ± 0.7	17	27.8 ± 1.2
2.2	10.8 ± 0.7	20	16.6 ± 1.1	1.8	16.5 ± 0.7	18	28.2 ± 1.3
2.5	12.5 ± 0.8	22	17.5 ± 1.0	2.0	16.9 ± 0.8	19	28.8 ± 1.2
2.8	12.4 ± 0.8	25	17.2 ± 1.1	2.2	17.2 ± 0.8	20	29.6 ± 1.3
3.1	12.3 ± 0.8	30	17.9 ± 1.1	2.5	18.6 ± 0.8	22	29.9 ± 1.2
3.4	12.6 ± 0.8	40	17.9 ± 1.1	2.8	19.2 ± 0.8	25	30.5 ± 1.2
3.7	12.2 ± 0.8	50	18.2 ± 1.2	3.1	19.9 ± 0.8	30	30.2 ± 1.2
4.0	12.3 ± 0.7	60	17.7 ± 1.1	3.4	21.2 ± 0.9	35	30.4 ± 1.2
4.5	12.5 ± 0.8	75	17.0 ± 1.1	3.7	22.5 ± 1.0	40	30.3 ± 1.2
5.0	13.2 ± 0.8	90	17.3 ± 1.0	4.0	25.5 ± 1.0	50	29.5 ± 1.2
5.5	13.1 ± 0.8	100	17.4 ± 1.2	4.5	26.7 ± 1.0	60	28.6 ± 1.2
6.0	13.4 ± 0.8	125	16.9 ± 1.0	5.0	27.1 ± 1.1	70	27.4 ± 1.1
6.5	13.7 ± 0.8	150	14.6 ± 0.9	5.5	27.6 ± 1.0	80	25.9 ± 1.1
7.0	13.3 ± 0.8	200	14.4 ± 1.0	6.0	27.2 ± 1.1	90	24.6 ± 1.0
7.5	14.0 ± 0.8	250	13.2 ± 0.9	6.5	27.3 ± 1.1	100	24.0 ± 1.0
8.0	14.1 ± 0.8	300	12.4 ± 1.0	7.0	28.6 ± 1.1	125	22.0 ± 0.9
8.5	13.8 ± 0.8	350	11.5 ± 1.0	7.5	29.1 ± 1.2	150	20.2 ± 0.9
9.0	14.4 ± 0.8	400	10.3 ± 0.8	8.0	29.5 ± 1.2	200	17.7 ± 0.7
9.5	14.6 ± 0.8	500	8.6 ± 0.6	8.5	30.8 ± 1.2	250	15.8 ± 0.7
10.0	14.5 ± 0.8	600	9.2 ± 0.6	9.0	30.6 ± 1.2	300	14.5 ± 0.6
11	14.5 ± 0.8			9.5	29.8 ± 1.2	350	13.3 ± 0.6
12	15.3 ± 0.9			10.0	29.4 ± 1.2	400	12.5 ± 0.5
13	15.8 ± 0.9			11	28.0 ± 1.1	500	10.7 ± 0.4
14	16.0 ± 1.0			12	27.1 ± 1.1	600	10.0 ± 0.4

the TCS values for CH_4 and CF_4 are around 60% of those of the three ethane-related molecules.

The positron TCS data in the range 20–150 eV are plotted in Fig. 7. In this region we can see the progress from the complicated behavior, due to the characteristic interaction in the positron–molecule system, to that due to the simple molecular size potential with increasing impact energies. In the energy region 30–150 eV the data sets of the TCS values for C_2F_6 versus those for CF_4, and the TCS values for C_2H_6 versus those for CH_4, respectively show a similar tendency. The TCS data of $C_2H_3F_3$ show a behavior roughly midway between those of C_2H_6 and C_2F_6. As shown in Figs. 4 and 7, the C_2F_6 TCS curve is not smooth. The vibrational feature may not be true, but erroneous.

Fig. 8 shows the electron TCS data of C_2F_6 for the present, Szmytkowski et al. [3] and Sanabia et al. [4] works, and the ICS data of Takagi et al. [2]. The present experimental data agrees well with the data of Sanabia et al. The three data sets for the electron TCS measurements show roughly the same large structures: peaks at 5, 9 and 30 eV, and a distinct valley at 14 eV in the TCS curve, although the TCS values does not coincide with each other. On the ICS data for elastic scattering (including rotational excitations) of Takagi et al., the maximum at 15 eV is greater than our (and those of Sanabia et al.) TCS values. The ICS data may be too large, at least above 10 eV.

The electron TCS data for C_2F_6 and $C_2H_3F_3$ for energies below 20 eV are plotted together with the data for C_2H_6 [6], CF_4 [7] and CH_4 [6] in Fig. 9. For molecules involving the F-atom, C_2F_6, $C_2H_3F_3$ and CF_4, there are one or two peaks in the region below the main peak at 5–10 eV. On the

Table 2
TCSs (10^{-16} cm^2) for positrons and electrons colliding with $C_2H_3F_3$ (the errors are the total uncertainties in the text)

Positron				Electron			
E (eV)	TCS	E (eV)	TCS	E (eV)	TCS	E (eV)	TCS
0.7	10.8 ± 0.6	15	15.3 ± 0.9	0.8	30.9 ± 0.8	13	26.9 ± 0.7
1.0	12.0 ± 0.7	16	15.7 ± 1.0	1.0	31.5 ± 0.7	14	26.0 ± 0.8
1.3	13.2 ± 0.7	17	16.6 ± 1.1	1.2	31.0 ± 0.6	15	25.7 ± 0.7
1.6	13.5 ± 0.8	18	16.1 ± 1.0	1.4	30.5 ± 0.6	16	25.2 ± 0.7
1.9	14.9 ± 0.8	19	16.3 ± 1.0	1.6	30.1 ± 0.6	17	25.5 ± 0.7
2.2	15.0 ± 0.8	20	17.0 ± 1.0	1.8	31.0 ± 0.6	18	24.5 ± 0.7
2.5	14.4 ± 0.8	22	16.3 ± 1.0	2.0	30.8 ± 0.7	19	26.5 ± 0.7
2.8	14.9 ± 0.8	25	16.9 ± 1.1	2.2	29.6 ± 0.6	20	26.3 ± 0.7
3.1	13.9 ± 0.8	30	17.6 ± 1.0	2.5	28.9 ± 0.6	22	26.0 ± 0.5
3.4	13.5 ± 0.8	40	17.0 ± 1.0	2.8	29.0 ± 0.6	25	25.8 ± 0.5
3.7	13.7 ± 0.8	50	16.2 ± 1.0	3.1	28.7 ± 0.7	30	24.5 ± 0.5
4.0	13.9 ± 0.7	60	15.9 ± 0.9	3.4	28.9 ± 0.7	35	22.5 ± 0.5
4.5	13.6 ± 0.7	70	15.5 ± 0.9	3.7	29.7 ± 0.7	40	22.6 ± 0.5
5.0	14.2 ± 0.8	80	14.8 ± 0.9	4.0	30.4 ± 0.7	50	20.5 ± 0.5
5.5	14.4 ± 0.8	90	14.9 ± 0.9	4.5	32.9 ± 0.8	60	20.1 ± 0.5
6.0	13.6 ± 0.8	100	14.1 ± 0.9	5.0	33.5 ± 0.8	70	20.3 ± 0.4
6.5	14.0 ± 0.8	120	13.7 ± 0.9	5.5	35.5 ± 0.8	80	19.1 ± 0.5
7.0	13.3 ± 0.7	150	12.5 ± 0.8	6.0	34.5 ± 0.8	90	18.2 ± 0.4
7.5	13.3 ± 0.7	200	11.7 ± 0.8	6.5	34.8 ± 0.8	100	17.7 ± 0.4
8.0	13.6 ± 0.8	250	10.5 ± 0.7	7.0	33.4 ± 0.8	125	15.8 ± 0.2
8.5	14.1 ± 0.8	300	9.6 ± 0.6	7.5	32.3 ± 0.8	150	14.4 ± 0.2
9.0	13.7 ± 0.8	400	8.8 ± 0.7	8.0	31.6 ± 0.9	200	12.7 ± 0.2
9.5	13.9 ± 0.8	500	7.6 ± 0.5	8.5	31.9 ± 0.8	250	11.6 ± 0.2
10.0	14.0 ± 0.7	600	6.7 ± 0.4	9.0	30.9 ± 0.8	300	10.5 ± 0.1
11	14.2 ± 0.8			9.5	29.9 ± 0.9	400	8.8 ± 0.1
12	14.9 ± 0.9			10.0	29.9 ± 0.8	500	7.7 ± 0.1
13	15.3 ± 0.9			11	28.9 ± 0.7	600	7.1 ± 0.1
14	15.7 ± 0.9			12	27.0 ± 0.8		

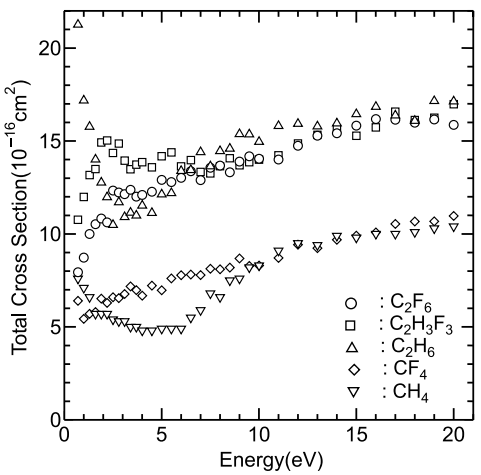

Fig. 6. TCSs for positrons with energies below 20 eV colliding with C_2F_6, $C_2H_3F_3$, C_2H_6, CF_4 and CH_4.

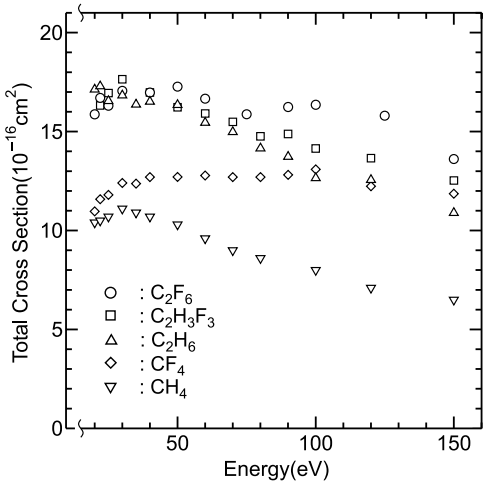

Fig. 7. TCSs for positrons with energies 15–150 eV colliding with C_2F_6, $C_2H_3F_3$, C_2H_6, CF_4 and CH_4.

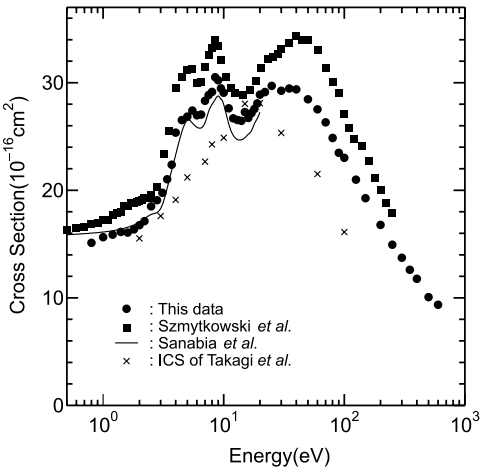

Fig. 8. TCSs for electrons colliding with C_2F_6 together with the TCS data of Szmytkowski et al. [3] and those of Sanabia et al. [4] and the ICSs of the elastic DCS data of Takagi et al. [2].

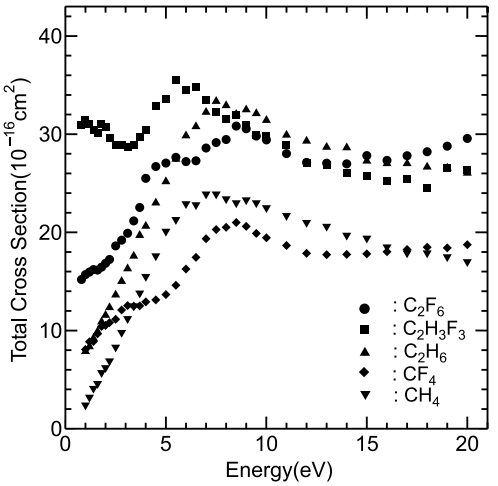

Fig. 9. TCSs for electrons with energies below 20 eV colliding with C_2F_6, $C_2H_3F_3$,C_2H_6, CH_4 and CF_4.

other hand, in C_2H_6 and CH_4 there is no structure in the low energy region. A weak hump in the C_2F_6 data is seen at 2.4 eV. The electron data for C_2F_6, for energies 5.5–14.0 eV, are lower than those for C_2H_6. The significant difference between the positron and electron data for $C_2H_3F_3$ is seen at energies lower than 4 eV.

Fig. 10 shows various electron TCS data for energies 20–150 eV. In the higher energy region, the order of the molecular size potential; C_2F_6, $C_2H_3F_3$, C_2H_6, CF_4 and CH_4, better determines the electron TCS sizes than the case of positron scattering shown in Fig. 7. However, the electron TCS values for CF_4, C_2F_6 and $C_2H_3F_3$ decrease more sharply, than their respective positron data, with increasing impact energies above 40 eV. The slopes above 60 eV for all molecules are roughly the same, different from the case of positron scattering shown in Fig. 7.

Ps formation cross sections are components of the TCSs for positron scattering in the range above the threshold energy E_{Ps} ($=7.7$ eV for C_2F_6 and 6.1 eV for $C_2H_3F_3$). As shown in Fig. 6, however, the increase of TCS due to Ps formation under a 9 G magnetic field (used for positron TCS measurements) is not directly visible. The orthodox method for the Ps formation cross section measurement [15] is not applicable with the present apparatus. As a result, an experiment under a stronger magnetic field (31 G) was performed to show the Ps formation cross section in the TCS curve. Under large forward scattering effects, the cross section for positrons, except Ps formation, decreases from the normal TCS values. Only the Ps formation cross section is not affected by the magnetic field due to positrons annihilation before reaching the detector. The Ps formation cross section at 2 eV above the threshold E_{Ps} is estimated using the method described previously [8]. The

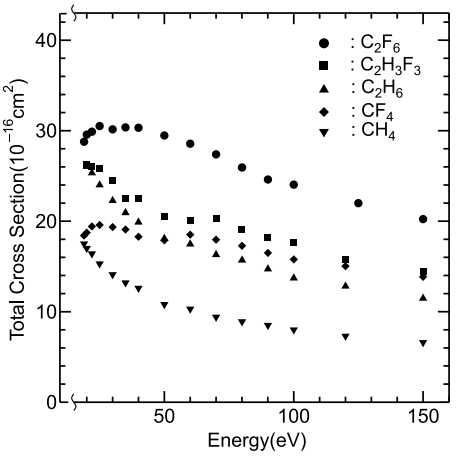

Fig. 10. TCSs for electrons with energies 15–150 eV colliding with C_2F_6, $C_2H_3F_3$, C_2H_6, CH_4 and CF_4.

cross section, Q_{Ps}, is 0.68×10^{-16} cm^2 for C_2F_6 and 0.58×10^{-16} cm^2 for $C_2H_3F_3$, respectively. The ratio of this value to the TCS, Q_{Ps}/Q_t, is about 4.5% and 4.0% for C_2F_6 and $C_2H_3F_3$, respectively. Corresponding to these values, the ratio value for C_2H_6 is 23% [8]. The ratio for C_2F_6 is much lower than those for He and H_2 [16]. As pointed out in our previous paper [8], the Q_{Ps} values for fluorinated hydrocarbons such as CF_4, C_2F_6, C_3F_8 are smaller by a factor of 4–5 than those for their hydrocarbon counterparts (CH_4, C_2H_6, C_3H_8). The Q_{Ps} value for $C_2H_3F_3$ is not midway between the values for the fluorinated-carbon group and that for the hydrocarbon group, but is rather closer to that for the former.

4. Discussion

The main purpose of this report is to present the positron and electron TCS data. In order to compare the TCS data for positrons and electrons, ratios of the positron TCS data for C_2F_6 and $C_2H_3F_3$ to the corresponding electron TCS data, Q_t^+/Q_t^- are plotted in Fig. 11 together with the ratios for C_2H_6. In the region 4–14 eV, the ratios for the three molecules are roughly same, being 0.4–0.6. The reason for the coincidence is unknown. From the characteristics of the ratio curves for C_2F_6 and $C_2H_3F_3$ below 4 eV and above 14 eV, a C_2F_6 molecule shows a typical C–F molecule characteristic whereas this is not so with $C_2H_3F_3$. That is, the characteristics of C–F molecules include a large value of the Q_t^+/Q_t^- ratio at low energies, and a large ratio value at large energies where the resonance effect in electron scattering is negligible [8]. Large ratio values at low energies for C_2H_6 are due to the low values of the electron TCS, just like those for CH_4. The feature resembling a large peak at around 8 eV is a common characteristic of polyatomic molecules. As mentioned in the discussion related to Figs. 6 and 9, the shape of the TCS curve for a molecule involving an F-atom, like C_2F_6, $C_2H_3F_3$ or CF_4, is not simple below about 5 eV.

At the high impact energy of 600 eV, the merging of TCSs for positron and electron for C_2F_6 is not observable yet. That is, the merging

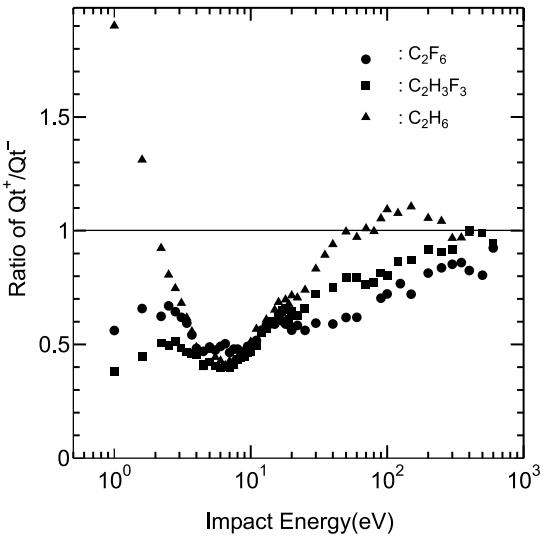

Fig. 11. Ratios of positron TCSs to electron TCSs, Q_t^+/Q_t^-, for C_2F_6, $C_2H_3F_3$ and C_2H_6.

phenomena for C_2F_6 do not exist in the range below 600 eV. The situation is the same for C_3F_8 [17] and CF_4 [7]. The positron TCS data for $C_2H_3F_3$ approach the electron data with increasing impact energy as shown in Figs. 5 and 11. On the merging phenomena, the $C_2H_3F_3$ molecule belongs to a kind of alkane molecules such as CH_4, C_2H_6 or C_3H_8.

It is noticeable in electron scattering that the present TCS data for C_2F_6 and $C_2H_3F_3$ are lower than those for C_2H_6 in the range between 5 and 15 eV. This tendency is quite similar to that in positron scattering. It may not be only due to the reason that the resonant states for C_2F_6 are weaker than those for C_2H_6. A similar tendency is seen in the relationship between CF_4 and CH_4. As described in the explanation related to Fig. 10, the polarization effect in polyatomic molecules involving fluorine atoms is very large. The ratio of the electron TCS values for C_2F_6 to those for C_2H_6 in the region 50–150 eV is roughly 2, and the same ratio for CF_4 to CH_4 is also roughly 2. On the contrary, TCSs for C_2F_6 are lower, between 5 and 15 eV, than those for C_2H_6 and the two are comparable below 20 eV. These tendencies at high and low energies are also the same for positron scattering. Above 20 eV the ratio Q_t^+/Q_t^- is in the order C_2H_6, $C_2H_3F_3$ and C_2F_6. It shows a noticeable

relationship to the basic interaction of positron or electron with atomic electrons.

We now discuss the data of 1,1,1-trifluoroethane ($C_2H_3F_3$). Because this molecule has a dipole moment, the forward scattering ratio is lager than those shown in Fig. 3 especially at low energies. Perhaps the ratio of the forward scattering cross section to the TCS may be about 10%. The correction values for the forward scattering effects to the measured TCS values are several percent, as shown in the figures and table. These values are rather small like those in SiH_4. The ratio of the correction is higher in the range above 100 eV for positrons and electrons. The electron DCS for C_2F_6 does not show strong forward peaking such as in CH_4 and SiH_4.

Acknowledgements

The authors would like to thank Dr. Akira Hamada and Mr. Hideki Takaki for their kind help in the initial stages of the measurements for C_2F_6.

References

[1] M. Kimura, Y. Itikawa (Eds.), Electron Collisions with Molecules on Gases: Applications to Plasma Diagnostics and Modeling, Adv. At. Mol. Opt. Phys. 44 (2001); L.G. Christophorou, J.K. Olthoff, M.V.V.S. Rao, J. Phys. Chem. Ref. Data 25 (1996) 1341.
[2] T. Takagi, L. Boesten, H. Tanaka, M.A. Dillon, J. Phys. B 27 (1994) 5389.
[3] C. Szmytkowski, P. Mozejko, G. Kasperski, E. Ptasinska-Denga, J. Phys. B 33 (2000) 15.
[4] J.E. Sanabia, G.D. Cooper, J.A. Tossell, J.H. Moore, J. Chem. Phys. 108 (1998) 389.
[5] L.G. Christophorou, J.K. Olthoff, J. Phys. Chem. Ref. Data 27 (1998) 1.
[6] O. Sueoka, S. Mori, J. Phys. B 19 (1986) 4035.
[7] O. Sueoka, S. Mori, A. Hamada, J. Phys. B 27 (1994) 1453.
[8] O. Sueoka, M. Kawada, M. Kimura, Nucl. Instr. and Meth. B 171 (2000) 96.
[9] O. Sueoka, H. Takaki, A. Hamada, M. Kimura, in: F. Aumayer, G. Betz, H.P. Winter (Eds.), 20th ICPEAC Abstracts Vol 1, WE05, Vienna 1997.
[10] K.R. Hoffman, M.S. Dababneh, Y.-F. Hsieh, W.E. Kauppila, V. Pol, J.H. Smart, T.S. Stein, Phys. Rev. A 25 (1982) 1393.
[11] S. Mori, O. Sueoka, J. Phys. B 27 (1994) 4349.
[12] P.G. Coleman, T.C. Griffith, G.R. Heyland, Appl. Phys. 5 (1974) 223.
[13] A. Hamada, O. Sueoka, J. Phys. B 27 (1994) 5055.
[14] H. Tanaka, L. Boesten, D. Matsunaga, T. Kudo, J. Phys. B 21 (1988) 1255.
[15] L.S. Fornari, L.M. Diana, P.G. Coleman, Phys. Rev. Lett. 51 (1983) 2276; S. Zhou, H. Li, W.E. Kauppila, C.K. Wan, T.S. Stein, Phys. Rev. A 55 (1997) 361.
[16] L.M. Diana, P.G. Coleman, D.L. Brooks, P.K. Pendleton, D.M. Narman, Phys. Rev. A 34 (1986) 2731.
[17] H. Tanaka, Y. Tachibana, M. Kitajima, O. Sueoka, H. Takaki, A. Hamada, M. Kimura, Phys. Rev. A 59 (1999) 2006.